Environmental and Molecular Mutagenesis 45:000–000 (2005)

Research Article

In Vivo Mutagenesis Induced by Benzo[*a*]pyrene Instilled Into the Lung of *gpt* delta Transgenic Mice

Akiko H. Hashimoto,[1] Kimiko Amanuma,[1] Kyoko Hiyoshi,[1,2] Hirohisa Takano,[1] Ken-ichi Masumura,[3] Takehiko Nohmi,[3] and Yasunobu Aoki[1]*

[1]*Research Center for Environmental Risk, National Institute for Environmental Studies, Ibaraki, Japan*
[2]*Graduate School of Comprehensive Human Sciences, University of Tsukuba, Ibaraki, Japan*
[3]*Division of Genetics and Mutagenesis, National Institute of Health Sciences, Tokyo, Japan*

Benzo[*a*]pyrene (B[*a*]P) is a ubiquitous airborne pollutant whose mutagenicity has been evaluated previously by oral and intraperitoneal administration to experimental animals. In this study, mutagenesis in the lungs, the target organ of air pollutants, was examined after a single intratracheal instillation of 0–2 mg B[*a*]P into *gpt* delta transgenic mice. Intratracheal injection of B[*a*]P resulted in a statistically significant and dose-dependent increase in *gpt* mutant frequency as measured by 6-thioguanine selection. The mutant frequencies at B[*a*]P doses of 0.5, 1, and 2 mg were 2.8, 4.2, and 6.8 times higher than the frequency seen in nontreated mice ($0.60 \pm 0.13 \times 10^{-5}$). The most frequent mutations induced by B[*a*]P treatment were G:C→T:A transversions, which are characteristic of B[*a*]P mutagenesis in other models, and single-base deletions of G:C base pairs. To characterize the hotspots of B[*a*]P-induced mutations in the *gpt* gene, we analyzed sequences adjacent to the mutated G:C base pairs. Guanine bases centered in the nucleotide sequences CGT, CGA, and CGG were the most frequent targets of B[*a*]P. Our results indicate that intratracheal instillation of B[*a*]P into *gpt* delta mice causes a dose-dependent increase in *gpt* mutant frequency in the lung, and that the predominant mutation induced is G:C→T:A transversion. Environ. Mol. Mutagen. 45:000–000, 2005. © 2005 Wiley-Liss, Inc.

Key words: benzo[a]pyrene; *gpt* delta transgenic mouse; 6-thioguanine selection

INTRODUCTION

Benzo[*a*]pyrene (B[*a*]P), one of the most potent mutagens in ambient air, is generated by the combustion of fossil fuels such as occurs in diesel engines and industrial settings. This polycyclic aromatic hydrocarbon (PAH), also a component of cigarette smoke and burned foods, is carcinogenic in rodent cancer bioassays [Singh et al., 1998; Iwagawa et al., 1989]. B[*a*]P is converted to reactive intermediates, B[*a*]P diol epoxides. Of these intermediates, benzo[*a*]pyrene 7,8-diol-9,10-epoxide (BPDE) is the most mutagenic [Miller et al., 2000], but all of the B[*a*]P diol epoxide enantiomers are carcinogenic in mammals [Buening et al., 1978]. The metabolism of B[*a*]P is catalyzed in various tissues by mono-oxygenases of the cytochrome P-450 (CYP) 1A family. Expression of the genes encoding these mono-oxygenases is mediated by the arylhydrocarbon receptor, a ligand-dependent transcription factor to which B[*a*]P and related PAHs bind. BPDE and other reactive metabolites are known to form DNA adducts, predominantly by binding to the exocyclic amino groups of guanine and adenine [Cosman et al., 1992; Bartsch, 1996]. The metabolites produced in the lung are qualitatively similar to those found in the liver and other tissues [Cohen et al., 1976; Prough et al., 1979; International Programme on Chemical Safety, 1998].

DNA adducts can cause mispairing of DNA bases, leading to the induction of mutations through the DNA

Grant sponsor: The Japan Society for the Promotion of Sciences; Grant number: 14207100.

*Correspondence to: Yasunobu Aoki, National Institute for Environmental Studies, 16-2 Onogawa, Tsukuba, Ibaraki 305-8506, Japan. E-mail: ybaoki@nies.go.jp

Received 21 May 2004; provisionally accepted 26 June 2004; and in final form 10 October 2004

DOI 10.1002/em.20098

Published online in Wiley InterScience (www.interscience.wiley.com).

B[a]P administration. Their lungs were removed, frozen in liquid nitrogen, and stored at −80°C until the DNA was isolated.

DNA Isolation and In Vitro Packaging of DNA

High-molecular-weight genomic DNA was extracted from the lungs using the RecoverEase DNA Isolation Kit (Stratagene, La Jolla, CA). Lambda EG10 phages were rescued using Transpack Packaging Extract (Stratagene).

gpt Mutation Assay

The *gpt* mutagenesis assay was performed according to previously described methods [Nohmi et al., 2000]. To convert the phage DNA into plasmids, *E. coli* YG6020 expressing Cre recombinase was infected with the rescued phage. The bacteria were then spread onto M9 salts plates containing Cm and 6-TG [Nohmi et al., 2000], which were incubated for 72 hr at 37°C for selection of the colonies harboring a plasmid carrying the chloramphenicol acetyltransferase (*cat*) gene and a mutated *gpt* gene. The 6-TG-resistant colonies were streaked onto selection plates for confirmation of the resistant phenotype. The cells were then cultured in LB broth containing 25 μg/ml of Cm at 37°C and collected by centrifugation. The bacterial pellets were stored at −80°C until DNA sequencing analysis was performed. Mutant frequencies for the *gpt* gene were calculated by dividing the number of colonies growing on M9 + Cm + 6-TG agar plates by the number of colonies growing on M9 + Cm agar plates.

PCR and DNA Sequencing Analysis of 6-TG-Resistant Mutants

A 739 bp DNA fragment containing the *gpt* gene was amplified by PCR using primer 1 (forward primer: 5′-TACCACTTTATCCCGCGTCAGG-3′) and primer 2 (reverse primer: 5′-ACAGGGTTTCGCTCAGGTTTGC-3′) [Nohmi et al., 2000]. The reaction mixture contained 5 pmole of each primer and 200 mM of each dNTP. PCR amplification was carried out using Ex Taq DNA polymerase (Takara Bio, Shiga, Japan) and performed with a Model PTC-100 Thermal Cycler (MJ Research, Waltham, MA). After the PCR products were purified, sequencing reactions were performed by using a DYEnamic ET Terminator kit (Amersham Biosciences, Piscataway, NJ). The sequencing primers were primer A (forward primer: 5′-GAGGCAGTGCGTAAAAAGAC-3′) and primer C (reverse primer: 5′-CTATTGTAACCCGCCTGAAG-3′) [Nohmi et al., 2000]. The sequencing reaction products were analyzed on an Applied Biosystems model 310 genetic analyzer (Applied Biosystems, Foster City, CA).

Statistical Analysis

All data are expressed as mean ± SD. Statistical significance was evaluated using ANOVA and the Scheffe test. $P < 0.05$ was considered to be statistically significant. To evaluate the linearity of the mutant frequency dose-response, a simple linear regression was performed. A statistical comparison of mutational spectra was performed using the Adams-Skopek test [Adams and Skopek, 1987; Cariello et al., 1994].

RESULTS

gpt Mutatnt Frequency in Lung of B[a]P-Treated Mice

To determine the mutagenic effects of B[a]P in the lung, *gpt* delta transgenic mice were exposed to increasing doses of B[a]P by intratracheal instillation. The body weights of mice given 0, 0.5, 1, and 2 mg B[a]P were 23.3 ± 0.9, 25.0 ± 0.0, 25.0 ± 0.6, and 24.5 ± 0.5 g, respectively, and there were no significant differences between the assay groups. The mutant frequency in the lungs of the control mice (0 mg B[a]P) was $0.60 \pm 0.13 \times 10^{-5}$ (n = 3). Single injections of 0.5, 1, and 2 mg resulted in increases in the mutant frequency of approximately 2.8-, 4.2-, and 6.8-fold ($1.7 \pm 0.22 \times 10^{-5}$, n = 3; $2.5 \pm 0.33 \times 10^{-5}$, n = 3; and 4.1×10^{-5}, n = 2), respectively, compared with the control mice (Table I). Mutation frequencies calculated from the mutant frequencies displayed similar fold increases. Significant differences were observed in the mutant and mutation frequencies between untreated and treated mice at the 1 and 2 mg doses but not at the 0.5 mg dose. The B[a]P treatment resulted in a significant linear dose-dependent increase in mutant frequency ($r^2 = 0.88$; $P < 0.001$; Fig. 1) and mutation frequency ($r^2 = 0.82$; $P < 0.01$; Fig. 1).

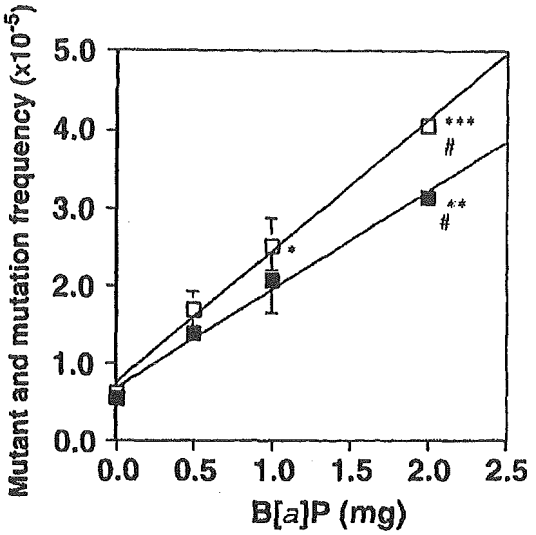

Fig. 1. 6-TG-induced mutant (open square) and mutation (filled square) frequency in the lungs of B[a]P-treated *gpt* delta mice. Data are expressed as mean ± SD (n = 3 for the control, 0.5 mg, and 1 mg groups; n = 2 for the 2 mg group). Number sign, average data of two animals. Statistical significance was determined using ANOVA and the Scheffe test. Significant differences between the control and B[a]P-induced groups are indicated: asterisk, $P < 0.05$; double asterisk, $P < 0.01$; triple asterisk, $P < 0.001$.

Characteristics of *gpt* Mutation Spectrum

To determine the spectrum of mutations caused by B[a]P instilled into the lung, 131 *gpt* mutants from the lungs of treated and control mice were subjected to DNA sequence analysis (Tables II and III). In control mice, 92% (12/13) of total mutations were base substitutions; G:C→C:G and G:C→T:A transversions and G:C→A:T transitions occurred at nearly equal frequencies. In the

TABLE III. DNA Sequence Analysis of *gpt* Mutations Obtained From the Lung of B[*a*]P-Treated and Untreated Control *gpt* delta Mice

Type of mutation	Nucleotide	Sequence change		Amino acid change	Total number of mutants (independent)[a]		Number of mutants									
							Control			B[*a*]P 0.5 mg			B[*a*]P 1 mg			B[*a*]P 2 mg	
					Control	B[*a*]P	Number 1	Number 2	Number 3	Number 1	Number 2	Number 3	Number 1	Number 2	Number 3	Number 1	Number 2
Base substitution																	
Transition																	
G:C→A:T	64	Cga→Tga	CpG	Arg→Stop		2 (1)						2					
	86	tGg→tAg		Trp→Stop		2								1		1	
	110	cGt→cAt	CpG	Arg→His	1	3 (2)	1									1	2
	115	Ggt→Agt	CpG	Gly→Ser		1								1			
	128	gGt→gAt		Gly→Asp		1										1	
	262	Gat→Aat		Asp→Asn	1				1								
	274	Gat→Aat		Asp→Asn	1			1									
	352	Ggt→Agt		Gly→Ser		1										1	
	402	tgG→tgA		Trp→Stop		1									1		
	409	Cag→Tag		Gln→Stop		1						1					
	418	Gat→Aat		Asp→Asn		1							1				
A:T→G:C	25	Tgg→Cgg		Trp→Arg	1			1									
	56	cTc→cCc		Leu→Pro	1	1		1			1						
	415	Tgg→Cgg		Trp→Arg		2 (1)										2	
Transversion																	
G:C→T:A	7	Gaa→Taa	CpG	Glu→Stop		3 (1)				3							
	108	agC→agA		Ser→Arg		2 (1)									2		
	110	cGt→cTt	CpG	Arg→Leu		3 (2)										2	1
	115	Ggt→Tgt	CpG	Gly→Cys		4 (3)									2	1	1
	116	gGt→gTt		Gly→Val		1				1							
	140	gCg→gAg	CpG	Ala→Glu		3									1	1	1
	143	cGt→cTt	CpG	Arg→Leu		10 (4)							1		7	1	1
	176	tGt→tTt		Cys→Phe		1											1
	185	aGc→aTc		Ser→Ile	1		1										
	186	agC→agA		Ser→Arg	1			1									
	189	taC→taA	CpG	Tyr→Stop		4 (3)							2		1		1
	208	Gag→Tag	CpG	Glu→Stop		4 (2)									3		1
	244	Gaa→Taa	CpG	Glu→Stop		10 (2)									2		8
	304	Gaa→Taa		Glu→Stop	1	1			1	1							
	402	tgG→tgT		Trp→Cys		2								1			1
	409	Cag→Aag		Gln→Lys		1										1	
	413	cCg→cAg	CpG	Pro→Gln		3				1					1	1	
G:C→C:G	50	cGt→cCt	CpG	Arg→Pro		1									1		
	108	agC→agG		Ser→Arg		1										1	
	112	Ggc→Cgc		Gly→Arg	1		1										
	125	cCg→cGg	CpG	Pro→Arg		2							1		1		
	143	cGt→cCt	CpG	Arg→Pro		1											1
	186	agC→agG		Ser→Arg	2 (1)	1	2								1		
	206	cGc→cCc	CpG	Arg→Pro		1										1	

(*Continued*)

B[*a*]P-treated group, 44% of the mutations (52/118) were G:C→T:A transversions, and 14% (16/118) were one-base deletions. A dose-dependent increase in base deletions was observed in the range of 0–2 mg B[*a*]P, while G:C→T:A transversions increased with dose at 0.5–1 mg B[*a*]P, but decreased slightly at 2 mg B[*a*]P.

The mutational analysis data were used to estimate mutation frequency. Mutations that were isolated more than once from an individual mouse were considered to be the result of clonal expansion and counted as a single independent mutation. Using this correction, 92% (12/13) of control mutations were independent, while 74% (87/118) of mutations from treated mice were independent. For most types of mutations, independent mutations and total mutations displayed very similar distributions (Table II), and mutant frequency and mutation frequency had very similar dose-response relationships (Fig. 1, Table I). Marked differences between mutant frequency and mutation frequency, however, were observed for G:C→T:A transversions. The mutant frequency for G:C→T:A transversion was estimated to be 0.11×10^{-5} (control), 0.61×10^{-5} (0.5 mg B[*a*]P), 1.4×10^{-5} (1 mg B[*a*]P), and 1.3×10^{-5} (2 mg B[*a*]P), as shown in Figure 2. On the other hand, the mutation frequency for G:C→T:A transversion was estimated to be 0.11, 0.41, 0.69, and 0.82×10^{-5} for 0, 0.5, 1, and 2 mg of B[*a*]P, respectively. Although different, both the mutation frequency and mutant frequency for G:C→T:A transversion increased dose-dependently.

There was a significant difference between the mutation spectra shown in Table II for untreated mice and mice treated with 1 mg B[*a*]P ($P < 0.05$). The spectra for mice treated with 0.5 and 2 mg B[*a*]P, however, were not significantly different from the control spectrum ($P = 0.60$ and 0.056). Also, there was no significant difference between the control mutation spectrum and the spectrum of total B[*a*]P-induced mutations ($P = 0.10$) or between the spectrum of independent control mutations and either the spectrum of total B[*a*]P-induced independent mutations ($P = 0.09$) or the spectrum of independent mutations produced by each of the different doses of B[*a*]P ($P = 0.86$, 0.30, and 0.15).

The positions of *gpt* mutations induced by B[*a*]P are listed in Table III. Among the G:C→T:A transversions isolated from B[*a*]P-treated mice, five *gpt* mutations (at nucleotides 115, 140, 143, 189, and 413) were each observed in three or more mice; these positions therefore are potential hotspots for B[*a*]P mutation. Significant differences were observed for the hotspots in untreated and treated mice ($P < 0.05$, Adams-Skopek test).

The predominant frameshift mutation in B[*a*]P-treated mice was single-base pair deletion of G:C base pairs (15/16; 94%). Thirty-eight percent of single-base deletions (6/16) occurred at G:C sites in 5′-TGG-3′ sequences, and the deletion of G:C from a run of G:Cs occurred in 63% of −1 frameshifts (10/16; Table III). There were, however, no apparent hotspots for deletion.

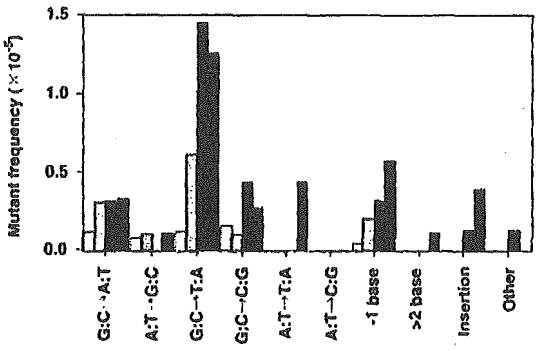

Fig. 2. Comparison of 6-TG-induced mutation spectra (not corrected for clonality) in control and B[*a*]P-treated *gpt* delta mice. Open bar, control; light gray bar, 0.5 mg; dark gray bar, 1 mg; closed bar, 2 mg.

DISCUSSION

To determine the mutant frequency and mutation spectrum induced by B[*a*]P in the lung, B[*a*]P was administered directly into the lungs of *gpt* delta mice. The mutagenicity of B[*a*]P has previously been determined in the liver, spleen, forestomach, and bone marrow using oral administration or i.p. injection in the Big Blue mouse [Skopek et al., 1996; Shane et al., 1997, 2000], Muta Mouse [Mientjes et al., 1996; Rompelberg et al., 1996; Hakura et al., 1998; Kosinska et al., 1999], and the *rpsL* transgenic mouse [Muto et al., 1999]. In these reports, the authors did not determine whether the mutant frequency depended on the dose of B[*a*]P except for one study using spleen T-cells [Skopek et al., 1996]. Our results indicate that the mutant frequency in the lung increases linearly with the dose of B[*a*]P. Therefore, when this compound is directly administered to a target organ, the lung, the amount of B[*a*]P bound to DNA in the form of a BPDE-DNA adduct appears to be proportional to the dose of B[*a*]P administered.

B[*a*]P administered by intratracheal injection also causes lung tumors in direct proportion to the total dose (0–8 mg) [Yoshimoto et al., 1983; Ide et al., 2000; Tchou-Wong et al., 2002]. For instance, the incidence of lung tumors was 39% at a dose of 4 mg B[*a*]P [Tchou-Wong et al., 2002]. These data indicate that lung tumors are induced under the same conditions and with a similar dose response as *gpt* mutations in *gpt* delta mice. Human B[*a*]P intake from air was estimated by Raiyani et al. [1993]. On the basis of an average inhalation of 15 m^3 air per day, exposure to B[*a*]P was calculated to be 0.19 μg/day in industrial areas [International Programme on Chemical Safety, 1998]. Therefore, the 1 mg dose of B[*a*]P used in this report is equivalent to the total intake of B[*a*]P received through inhalation over 14.4 years (5,263 days).

To analyze the spectrum of mutations caused by B[*a*]P in the lung, we determined the sequences of mutated *gpt* genes.

Cariello NF, Piegorsch WW, Adams WT, Skopek TR. 1994. Computer program for the analysis of mutational spectra: application to *p53* mutations. Carcinogenesis 15:2281–2285.

Cohen GM, Haws SM, Moore BP, Bridges JW. 1976. Benzo(a)pyren-3-yl hydrogen sulphate, a major ethyl acetate-extractable metabolite of benzo(a)pyrene in human, hamster and rat lung cultures. Biochem Pharmacol 25:2561–2570.

Cosman M, de los Santos C, Fiala R, Hingerty BE, Singh SB, Ibanez V, Margulis LA, Live D, Geacintov NE, Broyde S. 1992. Solution conformation of the major adduct between the carcinogen (+)-anti-benzo[*a*]pyrene diol epoxide and DNA. Proc Natl Acad Sci USA 89:1914–1918.

Denissenko MF, Pao A, Tang MS, Pfeifer GP. 1996. Preferential formation of benzo[*a*]pyrene adducts at lung cancer mutational hotspots in P53. Science 274:430–432.

Hakura A, Tsutsui Y, Sonoda J, Kai J, Imade T, Shimada M, Sugihara Y, Mikami T. 1998. Comparison between in vivo mutagenicity and carcinogenicity in multiple organs by benzo[*a*]pyrene in the *lacZ* transgenic mouse (Muta Mouse). Mutat Res 398:123–130.

Hakura A, Tsutsui Y, Sonoda J, Tsukidate K, Mikami T, Sagami F. 2000. Comparison of the mutational spectra of the *lacZ* transgene in four organs of the Muta Mouse treated with benzo[*a*]pyrene: target organ specificity. Mutat Res 447:239–247.

Ide F, Iida N, Nakatsuru Y, Oda H, Tanaka K, Ishikawa T. 2000. Mice deficient in the nucleotide excision repair gene *XPA* have elevated sensitivity to benzo[*a*]pyrene induction of lung tumors. Carcinogenesis 21:1263–1265.

International Programme on Chemical Safety. 1998. Selected non-heterocyclic polycyclic aromatic hydrocarbons: environmental health criteria 202.Geneva:World Health Organization. p267–276.

Iwagawa M, Maeda T, Izumi K, Otsuka H, Nishifuji K, Ohnishi Y, Aoki S. 1989. Comparative dose-response study on the pulmonary carcinogenicity of 1,6-dinitropyrene and benzo[*a*]pyrene in F344 rats. Carcinogenesis 10:1285–1290.

Kosinska W, von Pressentin MdM, Guttenplan JB. 1999. Mutagenesis induced by benzo[*a*]pyrene in *lacZ* mouse mammary and oral tissues: comparisons with mutagenesis in other organs and relationships to previous carcinogenicity assays. Carcinogenesis 20: 1103–1106.

Masumura K, Matsui K, Yamada M, Horiguchi M, Ishida K, Watanabe M, Ueda O, Suzuki H, Kanke Y, Tindall KR, Wakabayashi K, Sofuni T, Nohmi T. 1999. Mutagenicity of 2-amino-1-methyl-6-phenylimidazo [4,5-*b*]pyridine (PhIP) in the new *gpt* delta transgenic mouse. Cancer Lett 143:241–244.

Masumura K, Matsui K, Yamada M, Horiguchi M, Ishida K, Watanabe M, Wakabayashi K, Nohmi T. 2000. Characterization of mutations induced by 2-amino-1-methyl-6-phenylimidazo[4,5-*b*]pyridine in the colon of *gpt* delta transgenic mouse: novel G:C deletions beside runs of identical bases. Carcinogenesis 21:2049–2056.

Masumura K, Horiguchi M, Nishikawa A, Umemura T, Kanki K, Kanke Y, Nohmi T. 2003. Low dose genotoxicity of 2-amino-3,8-dimethylimidazo-[4,5-*f*]quinoxaline (MeIQx) in *gpt* delta transgenic mice. Mutat Res 541:91–102.

Mientjes EJ, Steenwinkel MJST, van Delft JHM, Lohman PHM, Baan RA. 1996. Comparison of the X-gal- and P-gal-based systems for screening of mutant λ *lacZ* phages originating from the transgenic mouse strain 40.6. Mutat Res 360:101–106.

Miller ML, Vasunia K, Talaska G, Andringa A, de Boer J, Dixon K. 2000. The tumor promoter TPA enhances benzo[*a*]pyrene and benzo[*a*]pyrene diolepoxide mutagenesis in Big Blue mouse skin. Environ Mol Mutagen 35:319–327.

Monroe JJ, Kort KL, Miller JE, Marino DR, Skopek TR. 1998. A comparative study of in vivo mutation assays: analysis of *hprt*, *lacI*, and *cIIlcI* as mutational targets for *N*-nitroso-*N*-methylurea and benzo[*a*]pyrene in Big Blue mice. Mutat Res 421:121–136.

Mullin AH, Nataraj D, Ren JJ, Mullin DA. 1998. Inhaled benzene increases the frequency and length of *lacI* deletion mutations in lung tissues of mice. Carcinogenesis 19:1723–1733.

Muto S, Yokoi T, Gondo Y, Katsuki M, Shioyama Y, Fujita K, Kamataki T. 1999. Inhibition of benzo[*a*]pyrene-induced mutagenesis by (−)-epigallocatechin gallate in the lung of *rpsL* transgenic mice. Carcinogenesis 20:421–424.

Nohmi T, Katoh M, Suzuki H, Matsui M, Yamada M, Watanabe M, Suzuki M, Horiya N, Ueda O, Shibuya T, Ikeda H, Sofuni T. 1996. A new transgenic mouse mutagenesis test system using Spi$^-$ and 6-thioguanine selections. Environ Mol Mutagen 28: 465–470.

Nohmi T, Suzuki T, Masumura K. 2000. Recent advances in the protocols of transgenic mouse mutation assays. Mutat Res 455:191–215.

Prough RA, Patrizi VW, Okita RT, Masters BSS, Jakobsson SW. 1979. Characteristics of benzo(a)pyrene metabolism by kidney, liver and lung microsomal fractions from rodents and humans. Cancer Res 39:1199–1206.

Raiyani CV, Jani JP, Desai NM, Shah JA, Kashyap SK. 1993. Levels of polycyclic aromatic hydrocarbons in ambient environment of Ahmedabad City. Ind J Environ Prot 13:206–215.

Rompelberg CJM, Steenwinkel MJST, van Asten JG, van Delft JHM, Baan RA, Verhagen H. 1996. Effect of eugenol on the mutagenicity of benzo[*a*]pyrene and the formation of benzo[*a*]pyrene-DNA adducts in the λ-*lacZ*-transgenic mouse. Mutat Res 369: 87–96.

Shane BS, Lockhart AMC, Winston GW, Tindall KR. 1997. Mutant frequency of *lacI* in transgenic mice following benzo[*a*]pyrene treatment and partial hepatectomy. Mutat Res 377:1–11.

Shane BS, de Boer J, Watson DE, Haseman JK, Glickman BW, Tindall KR. 2000. *LacI* mutation spectra following benzo[*a*]pyrene treatment of Big Blue mice. Carcinogenesis 21:715–725.

Singh SV, Benson PJ, Hu X, Pal A, Xia H, Srivastava SK, Awasthi S, Zaren HA, Orchard JL, Awasthi YC. 1998. Gender-related differences in susceptibility of A/J mouse to benzo[*a*]pyrene-induced pulmonary and forestomach tumorigenesis. Cancer Lett 128:197–204.

Skopek TR, Kort KL, Marino DR, Mittal LV, Umbenhauer DR, Laws GM, Adams SP. 1996. Mutagenic response of the endogenous *hprt* gene and *lacI* transgene in benzo[*a*]pyrene-treated Big Blue B6C3F1 mice. Environ Mol Mutagen 28:376–384.

Swiger RR, Cosentino L, Masumura K, Nohmi T, Heddle JA. 2001. Further characterization and validation of *gpt* delta transgenic mice for quantifying somatic mutations in vivo. Environ Mol Mutagen 37:297–303.

Takano H, Yanagisawa R, Ichinose T, Sadakane K, Inoue K, Yoshida S, Takeda K, Yoshino S, Yoshikawa T, Morita M. 2002. Lung expression of cytochrome P450 1A1 as a possible biomarker of exposure to diesel exhaust particles. Arch Toxicol 76:146–151.

Tchou-Wong KM, Jiang Y, Yee H, LaRosa J, Lee TC, Pellicer A, Jagirdar J, Gordon T, Goldberg JD, Rom WN. 2002. Lung-specific expression of dominant-negative mutant p53 in transgenic mice increases spontaneous and benzo(a)pyrene-induced lung cancer. Am J Respir Cell Mol Biol 26:186–193.

Thybaud V, Dean S, Nohmi T, de Boer J, Douglas GR, Glickman BW, Gorelick NJ, Heddle JA, Heflich RH, Lambert I, Martus HJ, Mirsalis JC, Suzuki T, Yajima N. 2003. In vivo transgenic mutation assays. Mutat Res 540:141–151.

Yamada K, Suzuki T, Kohara A, Hayashi M, Hakura A, Mizutani T, Saeki K. 2002. Effect of 10-aza-substitution on benzo[*a*]pyrene mutagenicity in vivo and in vitro. Mutat Res 521:187–200.

Yoshimoto T, Inoue T, Iizuka H, Nishikawa H, Sakatani M, Ogura T, Hirao F, Yamamura Y. 1980. Differential induction of squamous cell carcinomas and adenocarcinomas in mouse lung by intratracheal instillation of benzo(a)pyrene and charcoal powder. Cancer Res 40:4301–4307.

ELSEVIER

Environmental Toxicology and Pharmacology 18 (2004) 21–37

ENVIRONMENTAL TOXICOLOGY AND PHARMACOLOGY
ETAP

www.elsevier.com/locate/etap

Dioxin health risk to infants using simulated tissue concentrations

Wakae Maruyama [a,*], Kikuo Yoshida [b], Yasunobu Aoki [a]

[a] *Research Center for Environmental Risk, National Institute for Environmental Studies, 16-2 Onogawa, Tsukuba 305-8506, Japan*
[b] *Research Center for Chemical Risk Management, National Institute of Advanced Industrial Science and Technology, 16-1 Onogawa, Tsukuba, Ibaraki 305-8569, Japan*

Received 4 December 2003; accepted 9 May 2004

Available online 26 June 2004

Abstract

Dioxin concentrations in infant and child were simulated using physiologically based pharmacokinetic (PBPK) models developed for these groups. The infant model was validated by comparing the simulated concentration with the measured concentration from the literature, and they showed good agreement. Simulations with our PBPK model showed temporal patterns in concentrations in various tissues. For risk assessment, estimated concentrations of 29 dioxins in the liver were summed up in a toxic equivalency (TEQ) basis to be compared with actual 2,3,7,8-TCDD concentrations in rat liver associated with toxicity. Maximum liver concentrations in breast-fed and formula-fed infants were 16.8 pg TEQ/g and 3.5 pg TEQ/g, respectively. The level in breast-fed infant liver was approximately 1/300 of the level associated with hepatocellular carcinoma and 1/5 of the level found in maternal rat liver associated with alterations in reproductive organs in the next generation. Based on our analysis, the present contamination level is not safe enough, but further dose–response data is required for a quantitative risk assessment.

Keywords: Dioxin; Risk; Human; Infant; PBPK model

1. Introduction

Our diets contain mixtures of dioxins that include polychlorinated dibenzo-*p*-dioxins (PCDDs), polychlorinated dibenzofurans (PCDFs) and coplanar polychlorinated biphenyls (CoPCBs) (Fries and Paustenbach, 1990; Guo et al., 2001). According to a study of total diet in Japan (Toyoda et al., 1999), adults consume about 152 pg TEQ (toxic equivalency) of dioxins per day, which is equivalent to about 2.5 pg TEQ/kg BW day (body weight per day). Since dioxins are lipophilic, they accumulate in the lipid portion of the body, and high concentrations are found in breast milk (Abraham et al., 1998; Beck et al., 1994a,b; Korner et al., 1993; Schecter et al., 1998; Tada et al., 1999), and the composition of dioxin congeners is different among countries. Consequently, infants take in more dioxins than adults on a kilogram body weight basis, and the health risks associated with this exposure are a public concern (Kreuzer et al., 1997; LaKind et al., 2001; Patandin et al., 1999).

In the risk assessment of dioxins, not only the administered dose but also the internal concentration is important as dosimetry, since accumulation patterns are different among species. For example, half-lives of dioxins are very different between rats (20 days) and humans (6–7 years), so dose–response data in an animal bioassay cannot be directly used for human risk assessment. When animal data are utilized, interspecies differences in administration, distribution, metabolism and excretion (ADME) of a chemical complicate risk assessments. In these cases, tissue dose (tissue concentration) is more appropriate for route-to-route, low dose and interspecies extrapolations. The physiologically based pharmacokinetic (PBPK) model is a useful tool for estimating these doses (Paustenbach, 2000) since it can predict tissue levels over time. PBPK models for 2,3,7,8-tetrachlorodibenzo-*p*-dioxin (TCDD) have been developed in mice (Leung et al., 1988), rats (Andersen et al., 1993; Leung et al., 1989; Wang et al., 1997), and adult humans (Kissel and Robarge, 1988; Lawrence and Gobas, 1997).

* Corresponding author. Tel.: +81 29 850 2695; fax: +81 29 850 2920.
E-mail address: maruw@nies.go.jp (W. Maruyama).

1382-6689/$ – see front matter © 2004 Elsevier B.V. All rights reserved.
doi:10.1016/j.etap.2004.05.003

Kirman et al. (2000) applied the PBPK model to assess the brain cancer risk of acrylonitrile and tried to characterize the dose–response relationship in the target organ (the brain) using bioassay data. Andersen and Dennison (2001) also proposed that the tissue dose (tissue concentration) based on interspecies extrapolation was appropriate for assessing the risks of environmental chemicals. Based on these concepts, we analyzed exposure to dioxins through breast milk and food and the accumulation pattern in the target tissue as the first step of assessing the health risk of dioxin to human infant. Estimating tissue levels in infants is difficult because they grow rapidly and dioxin levels in their tissues change during the growth period. In addition, the composition of food materials consumed changes with age, therefore, the amount of dioxin uptake by infant and child may change age-dependently, too. To solve this problem, we modified an adult PBPK model (Maruyama et al., 2003) for infants and children by introducing equations for time-dependent changes in tissue weight, amount of consumed milk and food materials. After validating the model and simulating tissue levels, the sum of TEQ of 29 dioxins was compared with actual TCDD concentrations in rat liver associated with hepatocellular carcinoma (Kociba et al., 1978) and reproductive effects (Gray et al., 1995, 1997). We also estimated the peak time of the concentration to predict the time of occurrence of possible toxicity.

2. Methods

2.1. Basic equations and parameters for PBPK model

The PBPK models for infant and child are based on a previous model (Maruyama et al., 2003) for adult human, and the compartments in the models are liver, kidney, fat, blood, muscle, richly perfused tissue (brain, spleen and lung) and skin (Fig. 1).

The mass balance equations used in the model are as follows.

Kidney, fat, muscle, skin and richly perfused tissue:

$$\frac{dC_i}{dt} = Q_i \times \frac{(C_{blood} - C_i/R_i)}{G_i} \quad (1)$$

Blood:

$$\frac{dC_{blood}}{dt} = \left\{ \frac{\begin{array}{l}(Q_{liver} \times C_{liver}/R_{liver}) + (Q_{fat} \times C_{fat}/R_{fat}) + (Q_{kidney} \times C_{kidney}/R_{kidney}) \\ + (Q_{muscle} \times C_{muscle}/R_{muscle}) + (Q_{rich} \times C_{rich}/R_{rich}) + (Q_{skin} \times C_{skin}/R_{skin}) - C_{blood} \times (Q_{liver} \\ + Q_{fat} + Q_{kidney} + Q_{muscle} + Q_{rich} + Q_{skin}) + D \times Abs\end{array}}{G_{blood}} \right\} \quad (2)$$

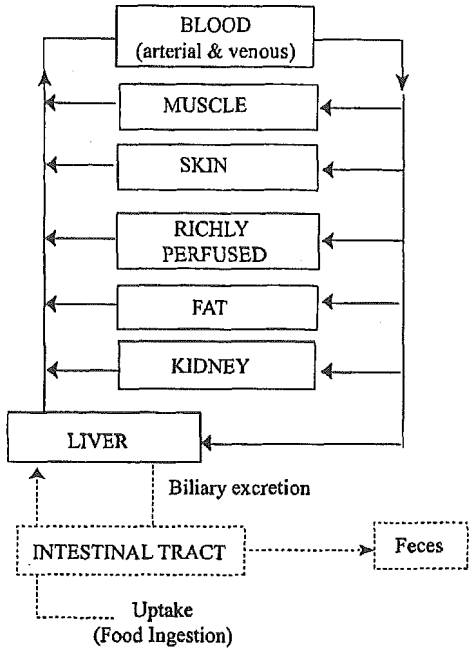

Fig. 1. Schematic diagram of the physiological model for humans. For the infant and child models, the volumes of the compartments increase time-dependently as described in Section 2.

Liver:

$$\frac{dC_{liver}}{dt} = \left\{ \frac{Q_{liver} \times (C_{blood} - C_{liver}/R_{liver}) - C_{liver} \times V_{liver} \times K_1}{G_{liver}} \right\} \quad (3)$$

Here Q_i is blood flow (mL/min), C_i is dioxin concentration (pg/g tissue), G_i is tissue weight, and R_i is the tissue–blood partition coefficient for tissue "i". C_{blood} is the dioxin concentration in blood.

Blood flow (Q_i) is also time-dependent and is expressed as follows using the blood perfusion rate (P_i) (mL/min-g), tissue volume (V_i) (mL) and compartment density (d_i) (g/mL) (Kissel and Robarge, 1988).

$$Q_i = P_i \times V_i \times d_i \quad (4)$$

$$Q_i = P_i \times G_i (G_i = V_i \times d_i) \quad (5)$$

Blood flow rates and tissue–blood partition coefficients for infants were the same as for adults. The compartment den-

Table 1
Concentration in breast and formula milk, gastrointestinal absorption (Abs) and daily amount of dioxins taken at age 1, 5, 10, 15 and 20, used to estimate tissue concentrations in a Japanese infant and child

	Concentration		Abs (%)	Amount of uptake via food (pg TEQ/day) at ages (years)				
	Breast milk[a] (pg/g)	Formula milk[b] (pg/g)		1	5	10	15	20
2378-TCDD	0.09	0.005	97	3.28	4.44	8.29	13.7	9.41
12378-PeCDD	0.22	0.02	99	6.09	8.43	13.5	19.9	15.1
123478-HeCDD	0.09	0.03	98	0.78	1.08	1.84	2.85	1.85
123678-HeCDD	0.88	0.04	97	1.03	1.43	2.33	3.50	2.44
123789-HeCDD	0.22	0.02	96	0.68	0.94	1.68	2.70	1.76
1234678-HpCDD	1.10	0.20	86	0.46	0.65	1.09	1.65	1.34
OCDD	11.4	0.32	76	0.03	0.04	0.11	0.20	0.13
2378-TCDF	0.04	0.005	97	0.94	1.28	2.09	3.16	2.86
12378-PeCDF	0.03	0.005	99	0.24	0.32	0.57	0.92	0.73
23478-PeCDF	0.54	0.04	98	5.55	7.77	11.7	16.3	13.4
123478-HeCDF	0.21	0.05	97	1.10	1.54	2.45	3.60	2.46
123678-HeCDF	0.42	0.05	97	1.06	1.48	2.35	3.45	2.32
123789-HeCDF	0.05	0.01	95	0.59	0.80	1.52	2.55	1.67
234678-HeCDF	0.22	0.12	96	1.79	2.54	3.55	4.60	3.12
1234678-HpCDF	0.25	0.19	87	0.30	0.43	0.59	0.75	0.55
1234789-HpCDF	0.05	0.03	100	0.08	0.11	0.18	0.28	0.19
OCDF	0.22	0.13	95	0.00	0.00	0.01	0.01	0.01
PCB77	0.97	0.05	99	0.00	0.01	0.01	0.02	0.01
PCB81	0.26	0.08	90	0.01	0.01	0.02	0.03	0.02
PCB126	2.65	0.20	99	12.0	16.5	25.6	37.0	33.6
PCB169	1.12	0.05	99	0.48	0.63	1.10	1.75	1.34
PCB105	74.7	3.00	99	0.37	0.51	0.77	1.08	1.12
PCB114	20.4	0.50	99	0.22	0.30	0.53	0.85	0.65
PCB118	340	11.0	99	1.38	1.90	2.85	3.99	4.12
PCB123	5.67	0.50	99	0.08	0.10	0.17	0.26	0.23
PCB156	112	1.00	99	0.72	0.98	1.56	2.29	2.16
PCB157	27.0	0.50	99	0.27	0.36	0.62	0.98	0.79
PCB167	37.9	0.50	99	0.02	0.03	0.04	0.06	0.06
PCB189	8.17	0.50	98	0.04	0.05	0.10	0.16	0.12

[a] Calculated by the authors from blood concentration in Japanese women, measured by the Ministry of Environment, Japan in 1998.
[b] Calculated by the authors from dioxin concentration in Japanese cow's milk, measured by Toyoda et al. (1999).

sities (d_i) of liver, kidney, fat, blood, muscle, skin and richly perfused tissue are 1.04, 1.05, 0.92, 1.06, 1.04, 1.1, and 1.04, respectively. G_i is also time-dependent and changes with age (Age) according to equations given later. The blood perfusion rates P_i (mL/min/g) of liver, kidney, fat, muscle, richly perfused tissue and skin are set at 0.197, 0.22, 0.018, 0.03, 0.469 and 0.024, respectively, based on blood content in tissues (Snyder et al., 1974).

D is the daily amount of dioxin uptake and Abs is the intestinal absorption rate. D is the sum of uptakes from milk and food consumed. The uptake from milk (D_{MILK}) is expressed by dioxin concentration in breast- or formula milk (C_{MILK}) and the amount of milk ingested (V_{MILK}). V_{MILK} was set in a time-dependent manner as described later.

$$D_{MILK} = C_{MILK} \times V_{MILK} \quad (6)$$

Gastrointestinal absorption is variable from 70 to 85% depending upon the lipophilicity of food materials (Neal et al., 1982). The US EPA sets 50% as the gastrointestinal absorption for humans (US EPA, 2000), although its reason for doing so is not clear. In this study, we obtained Abs values for 29 dioxins from several reports (Dahl et al., 1995; Liem and Theelen, 1997; McLachlan, 1993). Concentrations in breast- and formula milk and Abs are listed in Table 1.

The elimination constant from the liver (K_1) is set as below, using the lipid content of the liver (L_{liver}, 6.5%) and bile (L_{bile}, 1.9%), and biliary excretion rate (BILE) (mL/day).

$$K_1 = \frac{BILE \times L_{bile}}{L_{liver} \times V_{liver}} \quad (7)$$

K_1 is the ratio of the amount eliminated from the liver. In this model, BILE for infant ($BILE_{infant}$) changes with the change of body weight (BW) as described below. BILE for an adult human ($BILE_{adult}$) of 70 kg BW is set at 237.6 mL/day (Snyder et al., 1974).

$$BILE_{infant} = BILE_{adult} \times (BW_{infant}/70\,kg)^{0.8} \quad (8)$$

About urinary excretion, we tried a preliminary calculation in previous studies (Maruyama et al., 2002, 2003) and found that the elimination via urine is sufficiently small to be neglected.

The elimination constant of dioxins in the human body is difficult to determine, since no supporting or quantita-

tive data, such as concentration of metabolites in feces or decrease in the concentration of non-metabolized dioxin in tissues, are available for humans. Although half-life is often used for the elimination constant in a one-compartment model, elimination speed is considered to be different in different tissues and one fixed half-life cannot be applied to all tissues. Therefore it is not reasonable to use the same constant (half-life) in the PBPK model. In the previous rat PBPK models, metabolism of 2,3,7,8-TCDD is considered to relate to the induction of chtochrome p450s (CYPs) such as CYP1A1 and CYP1A2, and accumulation of dioxin in the liver is considered to relate to the binding protein CYP1A2 (Andersen et al., 1993; Carrier et al., 1995a,b; Kohn et al., 1993; US EPA, 2000; Wang et al., 1997). In the rat model, induction rates of CYPs and accumulation of TCDD in rat liver were set and validated using experimental data (Andersen et al., 1993, 1997; Kohn et al., 1993). However, CYPs do not give direct information about the amount of metabolite, and how the term of metabolic elimination is introduced in the mass balance equation is different among the literature. According to previous reports, the terms for metabolism and protein binding can be inserted into Eq. (3) as follows:Liver:

$$\frac{dC_{liver}}{dt} = \left\{ \frac{Q_{liver} \times (C_{blood} - Cf_{liver}/R_{liver}) - Cf_{liver} \times V_{liver} \times K_1 + Cb_{liver} - K_f \times Cf_{liver}}{G_{liver}} \right\} \quad (3')$$

where Cf_{liver} is the concentration of a free form of dioxin, and Cb_{liver} is a bound form. K_f is a metabolic elimination constant not directly related to the activity of enzymes (CYPs). Cb_{liver} is divided into three types of bound form, namely, AhR-TCDD, CYP1A2-TCDD and CYP1A1-TCDD, and the former two types are the main contributors.

However, the induction patterns of these proteins by other dioxin congeners are not known either in experimental animals or in humans, and no quantitative information is available about these proteins in the human body. It was not successful to introduce the same induction and binding constants for rats into our human PBPK model because of lack of information, and model validation was impossible. We need at least induction speed and dissociation constant of human CYPs to be introduced into human model. On the other hand, dioxin concentration in human tissue does not seem high enough to induce binding protein, as observed in experimental animals (Andersen et al., 1993), and non-metabolized dioxin levels in human feces were greater than uptake levels (Schrey et al., 1998; Rohde et al., 1999).

Strictly, elimination of dioxins is considered to be the summation of (1) degradation to completely different compounds, (2) fecal excretion of metabolized and non-metabolized forms and (3) urinary excretion of metabolized and non-metabolized forms. About dioxin, (1) is not probable, since dioxins are stable compounds both in the environment and an animal body, and degradation has not been reported either for animals or humans. Although metabolism in (2) and (3) is possible by hydroxylation or conjugation and some metabolites of dioxin has been detected in animals, the metabolites in human feces and urine have not been reported. About fecal excretion, dioxin concentration data in rat feces was suggested by Abraham et al. (1989) and 3–20% of administered dioxins (PCDDs and PCDFs) were excreted in feces within 7 days in a non-metabolized form. From these results, we assumed that absorbed dioxin could be excreted in feces in a non-metabolized form. When the route of dioxin transport from tissues to feces is considered, an excretion of liver lipid via bile is reasonable, since dioxins are very lipophilic and possibly exist in liver lipid or bile lipid. PCDD/Fs and PCB77, PCB126 and PCB169 are found in human bile, and the concentration ratios among congeners in bile are quite similar to the ratios in the liver (Kitamura et al., 1999).

Therefore, in this study, we assumed fecal excretion of a non-metabolized form via bile excretion as a route of dioxin elimination. This assumption is reasonable, and the elimination rate can be validated using simulated and measured amounts of excreted dioxin in infant feces (Abraham et al., 1994; Korner et al., 1993). Ideally, fecal excretion is the balance of non-absorbed dioxins in food and excreted dioxins via bile. However, these two dioxins cannot be separated quantitatively because of lack of information in humans. Re-absorption of dioxins by enterohepatic circulation is not considered in this model, because of lack of quantitative information about the 29 kinds of dioxins.

Time-dependency was introduced to correct for growth in BW, tissue weight, milk consumption, food consumption and dioxin concentration in breast milk. Age-dependent changes in BW and tissue weight were based on previous report (Snyder et al., 1974) and introduced to the model. Tissue weights were set as follows:

For infants: (the unit of age is "week".)

BW (kg): age × 0.144 + 3.961 (9)

Liver (g): BW × 23 + 21.4 (10)

Muscle (kg): BW × 0.25 (11)

Blood (g): BW × 58.2 + 142 (12)

Fat (kg): BW × 0.11 (13)

Kidney (g): BW × 6.2 + 3.8 (14)

Richly perfused tissue (g): BW × 95 + 35 (15)

For children: (the unit of age is "year".)

BW (kg): age × 2.86 + 6.12 (16)

Liver (g): age × 69.6 + 184 (17)

Muscle (kg): BW × 0.4 (18)

Blood (g): BW × 90.3 − 26.5 (19)

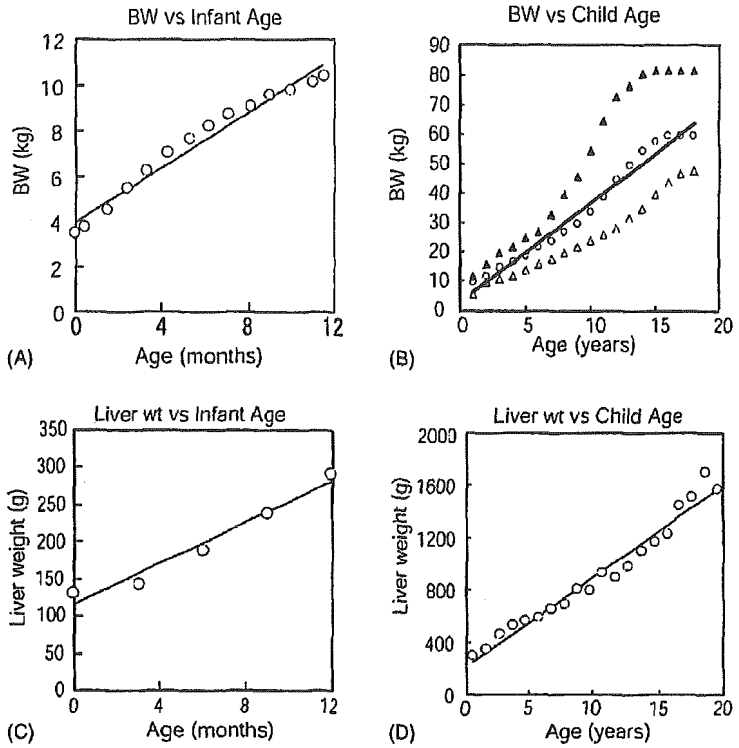

Fig. 2. Simulated (lines) for body weight (A and B) and liver weight (C and D) of infants (A and C) and children (B and D) in the model. Circles and triangles are the actual data obtained from the literature (Snyder et al., 1974).

$$\text{Fat (kg)}: \text{BW} \times 0.17 \quad (20)$$

$$\text{Kidney (kg)}: \text{age} \times 12.6 + 46.8 \quad (21)$$

$$\text{Richly perfused tissue (g)}: \text{age} \times 68 + 1158 \quad (22)$$

Although actual body and tissue weights do not increase according to these simple linear equations, body weights calculated with the equation were within the range of reference weights found in the literature (Snyder et al., 1974) (Fig. 2A and B) and calculated tissue weights also fitted the data found in the literature (Fig. 2C and D). BWs for a 1-year-old infant calculated from Eq. (9) (10.8 kg) and from Eq. (16) (8.98) do not match, due to the difference in the units of age and slope factors used in the equations. Considering these preliminary data, we used these equations in our model for time-dependency of body and tissue weight.

The concentrations of 29 dioxin congeners in Japanese breast milk used for simulation are listed in Table 1. The concentrations were calculated based on the blood concentration of Japanese women (Environment Agency, 2000). The concentration in formula milk was calculated from the dioxin concentration in cow's milk (Toyoda et al., 1999) and the lipid content of milk (3.8%). For a breast-fed infant, decrease in dioxin concentration in breast milk (C_{MILK}) was also taken into account in this model, since studies report a decrease in dioxin concentration in women's tissue during lactation (Abraham et al., 1998; Iida et al., 1999; LaKind et al., 2001; Schecter et al., 1998).

$$C_{MILK} = (1 - \text{age} \times 0.0125) \times C_0 \quad (23)$$

where C_0 is the initial dioxin concentration in breast milk on the 0th week, and the unit of age is weeks.

The amount of milk ingested (V_{MILK}) (mL) changed with age (week) as shown in Fig. 3A, according to a report by Tada et al. (1999). Uptake of dioxin via baby food was calculated from dioxin concentration in Japanese food materials (Toyoda et al., 1999) and food consumption rate via baby food (Table 2) (Sato et al., 1999). Time-dependent changes of dioxin uptake for an infant via breast milk, formula milk and baby food are shown in Fig. 3B in a toxic equivalency basis (pg WHO-TEQ/day).

The food consumption rates for males between 1 and 20 years of age (Table 2) were calculated based on the National Nutrition Survey of Japan (1998). Change in total uptake amount (pg WHO-TEQ/day) for a man of 1–20 years of age is shown in Fig. 3C, and the uptake amount of each congener used in the model is listed in Table 1.

2.2. Simulation of dioxin concentration

The PBPK model was built on Microsoft Excel 2000™ and sequential calculations were performed with an Excel macro function. Time courses over 48 weeks of the concentrations of 7 PCDDs, 10 PCDFs and 12 CoPCBs were simulated. The CoPCBs tested in this study were

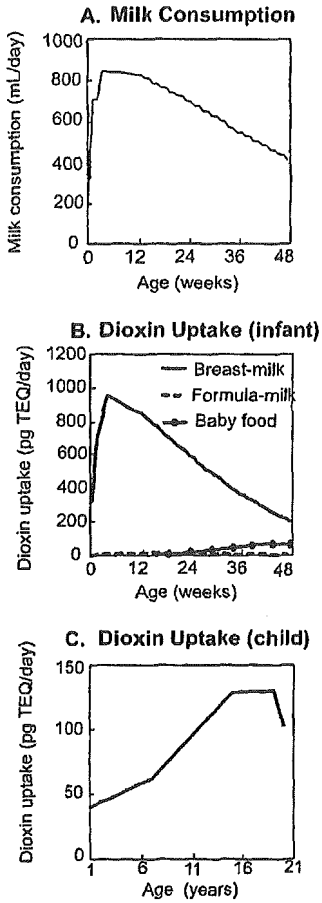

Fig. 3. (A) Daily amount of milk consumption (mL/day) used for simulation. (B) Daily uptake of dioxin (pg WHO-TEQ/day) by infants from breast milk (solid line), formula milk (broken line) and baby food (solid line with closed circle). (C) Daily uptake of dioxin (pg WHO-TEQ/day) for males between the ages of 1–20 years.

3,3′,4,4′-tetrachlorobiphenyl (TeCB) (PCB77), 3,4,4′,5-TeCB (PCB81), 3,3′4,4′,5-pentachlorobiphenyl (PeCB) (PCB126), 3,3′,4,4′,5,5′-hexachlorobiphenyl (HxCB) (PCB169), 2,3,3′,4,4′-PeCB (PCB105), 2,3,4,4′,5-PeCB (PCB114), 2,3′,4,4′,5-PeCB (PCB118), 2′,3,4,4′,5-PeCB (PCB123), 2,3,3′,4,4′,5-HxCB (PCB156), 2,3,3′,4,4′,5′-HxCB (PCB 157), 2,3′,4,4′,5,5′-HxCB (PCB167) and 2,3,3′,4,4′,5,5′-heptachlorobiphenyl (HpCB) (PCB189).

In this study, we focused on the exposure after birth and did not consider in utero exposure, and initial concentration in infant tissue was not set for simulation. In our preliminary calculation, setting initial concentration resulted in no apparent difference in tissue concentration. In the preliminary study, initial concentration was calculated using the dioxin concentration in breast milk and the ratio between dioxin concentrations in breast milk and fetus (Schecter et al., 1995). For children between the ages of 1 and 20 years, simulated tissue concentrations at 48 weeks of age were used as the initial concentrations.

Table 2
(A) Daily amount of food materials (g/day) assumed for an infant and (B) assumed daily food consumption (g/day) of children and young people

Food material	Age (month)				
	0–5	5–6	6–8	9–10	11–12
A					
Rice and cereals (dry)	0	7.0	26	72	84
Oil and fat	0	0.5	3.0	3.0	3.0
Fruits	0	12	17	35	45
Vegetables	0	23	33	70	90
Fish and shellfish	0	3.8	5.6	9.0	9.9
Meat and eggs	0	3.3	9.0	26	60
Dairy products	0	28	37	60	90
	Age (years)				
B	(1–6)	(7–14)	(15–19)	(20–29)	
Rice and cereals (dry)	102	168	370	338	
Oil and fat	6.1	9.0	23.7	21.6	
Fruits	59.6	64.3	92.4	77.8	
Vegetables and beans	73.0	124	215	224	
Fish and seafood	22.9	35.2	64.7	71.4	
Meat and eggs	41.3	68.3	153.9	139.2	
Milk and dairy product	97.4	165	146	93.6	
Sum (g)	734	1175	1241	811	

2.3. Validation

For validation, we simulated tissue concentrations in infants using dioxin concentration in breast milk (Table 3) and term of nursing (Table 4) and compared the simulated concentration to the measured concentration. Ideally, the data set should include the dioxin concentration data in breast milk and baby food, the term of breastfeeding, the dioxin concentration in the infant's tissue and the age of the infant at sampling time from a mother and her baby. While this data set is very difficult to obtain from humans, dioxin concentration in breast milk and food are sometimes available in the literature. Therefore, we prepared the concentration data sets for validation from different sources. We assumed that (1) dioxin concentration in maternal breast milk was similar among people in the same country over 5 years, (2) materials for baby food were not different between countries, and (3) the term of breastfeeding and the infant age at sampling were important for simulation and validation. We used 10 milk concentrations, simulated dioxin levels in infant liver, fat and blood, and compared these levels to 10 measured concentrations as listed in Table 4. Dioxin concentrations in feces were also used to validate elimination (Table 4).

2.4. Risk analysis

Since dioxins are lipophilic and accumulate in lipid portions of the body such as fat (adipose), internal concentration is preferred as dosimetry to evaluate health risk. The US EPA employed body burden to express internal dioxin level, and calculated benchmark dose and excess risk using estimated

Table 3
Dioxin concentrations in breast milk used for model simulation and validation

Data sources	Abraham (1998)					Beck (1994)	Korner (1993)		Abraham (1994)	
Data number	A1	A2	A3	A4	A5	B1, B2	C1	C2	D1	D2
Targeted tissue	Blood					Liver, fat	Feces		Feces	
2378-TCDD	0.07	0.06	0.05	0.07	0.05	0.02	0.14	0.08	0.06[a]	0.06
12378-PeCDD	0.20	0.15	0.19	0.20	0.14	0.46	0.59	0.21	0.26	0.24
123478-HeCDD	0.15	0.12	0.15	0.18	0.13	0.38	0.42	0.18	0.08[a]	0.08
123678-HeCDD	0.78	0.54	0.65	0.61	0.53	1.79	1.22	0.80	0.80	0.79
123789-HeCDD	0.08	0.07	0.12	0.10	0.10	0.34	0.48	0.20	0.06[a]	0.06
1234678-HpCDD	0.39	0.30	0.42	0.89	0.76	1.94	1.26	1.78	0.47	0.50
OCDD	1.96	1.48	3.89	3.54	5.60	13.1	4.82	6.86	1.99	2.20
2378-TCDF						0.10	0.05	0.10	0.03	0.03
12378-PeCDF						0.04	0.01	0.02	0.01	0.01
23478-PeCDF	0.52	0.35	0.34	0.47	0.30	0.76	0.20	0.45	0.68	0.64
123478-HeCDF	0.14	0.12	0.13	0.17	0.12	0.30	0.28	0.13	0.12	0.12
123678-HeCDF	0.11	0.08	0.09	0.11	0.09	0.30	0.21	0.14	0.12	0.14
123789-HeCDF							0.00	0.01[a]		
234678-HeCDF	0.04	0.04	0.04	0.06	0.04	0.11	0.16	0.07	0.03[a]	0.02
1234678-HpCDF	0.15	0.35	0.11	0.07	0.20	0.32	0.30	0.26	0.19	0.20
1234789-HpCDF							0.001[a]	0.001[a]		
OCDF						0.06	0.27	0.14	0.17	0.16
PCB77										
PCB81										
PCB126	2.79	2.40	3.68	5.36	4.03					
PCB169	3.43	2.76	5.81	3.50	2.52					
PCB105	0.08	0.10	0.16	0.32	0.10					
PCB114										
PCB118	0.60	0.25	0.84	1.17	0.66					
PCB123										
PCB156										
PCB157										
PCB167										
PCB189										

[a] Concentration was set as half of the detection limit.

Table 4
The sources of dioxin concentration in breast milk and tissues, terms of nursing and infant age used for simulation and validation

Data number[a]	Target tissue for validation	Data source for milk	Data source for tissues and feces	Term of breast-feeding (week)	Sampling age of infant (week)
A1	Blood	Abraham (1998)	Abraham (1998)	26	49
A2				29	48
A3				30	50
A4				32	52
A5				30	51
B1	Liver	Beck (1994b)	Beck (1994a)	21	39
B2	Fat			21	39
C1	Liver	Beck (1994b)	Kreuzer (1997)	6	44
C2				19	19
C3	Fat			6	44
C4				19	19
D1	Fecal excretion	Korner (1993)	Korner (1993)	3	3
D2				8	8
E1	Fecal excretion	Abraham (1994)	Abraham (1994)	20	20
E2				20	20

[a] The data numbers corresponds to the numbers in Table 3.

body burden. The merit of body burden is its convenience, since it can be calculated using a one-compartment model and the half-life of the dioxin. The demerit of body burden is that it is too simple an indicator and not sufficient to characterize the dose–response relationship in a target organ, and furthermore body burden cannot fully analyze route-to-route extrapolation. For example, the concentration of dioxin in rat liver is higher than the concentration based on lipid content, when the administered dose is high enough to induce dioxin-binding proteins in the liver (Abraham et al., 1988). Thus, body burden is rather an ambiguous indicator of internal level. Some researchers are still skeptical and request additional explanation of the use of body burden for interspecies scaling (US EPA, 2001). In addition, the method of calculating body burden is not uniform among researchers, and it is not clear whether body burden is calculated with a one-compartment model or calculated from measured concentration in blood or fat.

In this study, we selected liver concentration as a dose metric for interspecies extrapolation between animal and human. This assumption is based on the concept that the same concentration at the target organ brings the same adverse effect both for animal tissue and human tissue. For quantitative risk assessment, dose–response data at specific target organs is required, but these data are not available at present. Instead, we used the liver concentrations found at LOAEL (lowest-observed adverse effect level) associated with cancer (Kociba et al., 1978; Teeguarden et al., 1999; Tritscher et al., 1992) and reproductive toxicity (Faqi et al., 1998; Gray et al., 1995, 1997; Ohsako et al., 2001). Only liver concentrations were available as the common exposure marker in these reports. The liver concentration is often measured in animals and human and the mechanism of the cancer promotion activity of dioxins is well studied in the liver (Tritscher et al., 1992).

The relative risk of dioxin uptake for Japanese infants was calculated by comparing the simulated dioxin concentration in the infant liver to the measured concentration data in rat liver that showed abnormalities in previous reports (Table 5). The reason why we selected these four pieces of literature for toxicity data was that the liver concentrations were available in the same application dose conditions. Kociba's study is on cancer effect, Teeguarden's study is on cancer promotion activity, and the others are on non-cancer effects. Kirman et al. characterized the dose–response relationship for brain cancer risk by acrylonitrile at the target organ, and the brain concentrations were estimated with a PBPK model and application dose in the literature. In this study, intended to improve risk assessment, we used temporal concentration at a target organ. Area under the concentration curve (AUC) is often used to assess cancer risk, however, we simply calculate risk as the ratio of measured concentration in animal tissue and estimated concentration in human tissue, because of lack of supporting information about the relationship between cancer formation and the duration of exposure to dioxin.

Table 5
2,3,7,8-TCDD doses with which toxic responses were observed in rats

		2,3,7,8-TCDD in liver (pg/g)
Kociba (1978)	Alteration in porphyrin metabolism, squamous carcinoma, hepatocellular carcinoma (rat)	5100
Teeguarden (1999)	Promotion of hepatic foci in a DEN-treated rat's liver.	1670[a]
Faqi (1998)	Reduced sperm number (rat)	75 (maternal, GD21) 240 (fetal, weaning)
Gray (1997)	Reproductive toxicity to male offspring (rat)	368[b] (maternal), 6.2[b] (fetal)

[a] Liver concentration was obtained from Tritscher's report (1992).
[b] Liver concentrations were measured by Hurst et al. (2000) after dosage of the same amount of dioxin.

In this study, for the sum of toxic equivalencies (TEQs) of 29 kinds of dioxin congeners, we use two kinds of different TEQs based on different toxicity equivalent factors (TEFs). WHO-TEQ is calculated using WHO-TEF (Van den Berg et al., 1998). H4IIE-TEQ is calculated using H4IIE-TEF, which is based on an ethoxyresorufin-*O*-deethylase (EROD) activity assay using the H4IIE rat hepatoma cell line (Giesy et al., 1997). EROD activity is considered to be parallel to many toxic effects by dioxin-like compounds. Although WHO-TEF is well recognized to express the total toxicity of dioxin congeners, we did not use it, since WHO-TEF is based on administered dose and does not even distinguish the difference in half-lives between rodents and humans. WHO- and H4IIE-TEF values are listed in Table 6.

3. Results

3.1. Dioxin uptake for infant and child

The uptakes of dioxin by infants and males, as calculated in the WHO-TEQ basis, are shown in Fig. 3B and C, respectively. Uptake increased from age 1–20 years but decreased with age when calculated per kilogram-body weight basis (data not shown). Maximum uptake by a man of 1–20 years of age was 4.4 pg TEQ/kg BW day.

The maximum amount of dioxin uptake from breast milk was 960 pg TEQ/day in the 4th week. This amount was equivalent to 212 pg WHO-TEQ/kg BW day, which was approximately 80 times more than the adult's daily uptake (2.54 pg TEQ/kg BW day). The maximum uptake from formula milk was 88.2 pg TEQ/day, which is equivalent to 19.4 pg TEQ/kg BW day and approximately 8 times more than the uptake for adults. The uptake from baby food started from 6.74 pg TEQ/day (1.03 pg TEQ/kg BW day) on the 16th week and continuously increased to 40.9 pg TEQ/day on the 48th week (3.76 pg TEQ/kg BW day) as shown in Fig. 3B. Dioxin uptake from breast milk decreased after

Table 6
Toxic equivalent factors (TEQ) based on CYP1A1 induction using rat hepatoma cell-line (H4IIE-TEF) (Giesy et al., 1997) and WHO-TEF (Van den Berg et al., 1998)

	H4IIE-TEF	WHO-TEF
2378-TCDD	1.0	1.0
12378-PeCDD	4.2×10^{-1}	1.0
123478-HeCDD	8.3×10^{-2}	1.0×10^{-1}
123678-HeCDD	2.4×10^{-2}	1.0×10^{-1}
123789-HeCDD	3.4×10^{-2}	1.0×10^{-1}
1234678-HpCDD	2.3×10^{-2}	1.0×10^{-2}
OCDD	5.4×10^{-4}	1.0×10^{-4}
2378-TCDF	2.0×10^{-1}	1.0×10^{-1}
12378-PeCDF	2.0×10^{-1}	5.0×10^{-2}
23478-PeCDF	2.8×10^{-1}	5.0×10^{-1}
123478-HeCDF	2.0×10^{-2}	1.0×10^{-1}
123678-HeCDF	6.0×10^{-1}	1.0×10^{-1}
123789-HeCDF	2.0×10^{-1}	1.0×10^{-1}
234678-HeCDF	3.0×10^{-1}	1.0×10^{-1}
1234678-HpCDF	3.0×10^{-1}	1.0×10^{-2}
1234789-HpCDF	2.0×10^{-2}	1.0×10^{-2}
OCDF	0	1.0×10^{-4}
PCB 77	1.9×10^{-3}	1.0×10^{-4}
PCB 81	1.8×10^{-5}	1.0×10^{-4}
PCB 126	2.2×10^{-2}	1.0×10^{-1}
PCB 169	4.7×10^{-4}	1.0×10^{-2}
PCB105	1.2×10^{-5}	1.0×10^{-4}
PCB114	3.5×10^{-7}	5.0×10^{-4}
PCB118	1.0×10^{-7}	1.0×10^{-4}
PCB123	8.0×10^{-6}	1.0×10^{-4}
PCB156	9.0×10^{-6}	5.0×10^{-4}
PCB157	5.5×10^{-5}	5.0×10^{-4}
PCB167	1.5×10^{-5}	1.0×10^{-5}
PCB189	1.0×10^{-5}	1.0×10^{-4}

reaching a peak at the 4–5th week (Fig. 3A), because of the decrease in both of the amount of milk ingested and the dioxin concentration in breast milk. On the 48th week, the infant's body weight was approximately 10.8 kg, and the total dioxin uptake for the breast- and formula-fed infants were 21.8 and 7.7 pg TEQ/kg BW day, respectively.

Among the 29 dioxin congeners tested, the dominant contributors to dioxin uptake (pg TEQ/day) for breast-fed infants were 2,3,7,8-TCDD (5.78%), 1,2,3,7,8-PeCDD (24.5%), 1,2,3,6,7,8-HxCDD (9.4%), 2,3,4,7,8-PeCDF (17.6%), PCB126 (25.5%) and PCB118 (4.6%) (data not shown). Most of these dioxins were also dominant contributors to dioxin uptake for adults (Maruyama et al., 2002).

3.2. Simulation of tissue concentrations

Tissue concentrations were simulated for 29 dioxin congeners, and examples of 2,3,7,8-TCDD are shown in Fig. 4. The patterns of change in concentrations were similar among congeners, and the concentrations varied between tissues (data not shown). The concentration of 2,3,7,8-TCDD in the liver, kidney, blood and richly perfused tissue peaked on the 14th, 15th, 12th and 13th week, respectively (Fig. 4A, B, E, F). The simulated concentrations increased continuously in fat and muscle both for breast and formula-fed infants (Fig. 4C and D). In breast-fed infants, the maximum concentrations of 2,3,7,8-TCDD in tissues (pg/g) were 1.4 (liver), 1.8 (kidney), 1.6 (fat), 0.6 (blood), 2.2 (muscle) and 2.5 (richly). The corresponding concentrations in formula-fed infants were 0.1 (liver), 0.12 (kidney), 0.15 (fat), 0.04 (blood), 0.21 (muscle) and 0.17 (richly). The average tissue concentrations of 2,3,7,8-TCDD (pg/g) in a breast-fed infant in a year were 1.0 (liver), 1.3 (kidney), 1.1 (fat), 0.43 (blood), 1.5 (muscle), and 1.7 (richly). These results suggest that the time-dependent change in concentration is quite different among different tissues, and it is important to estimate dioxin concentration in the target organ in the risk assessment process.

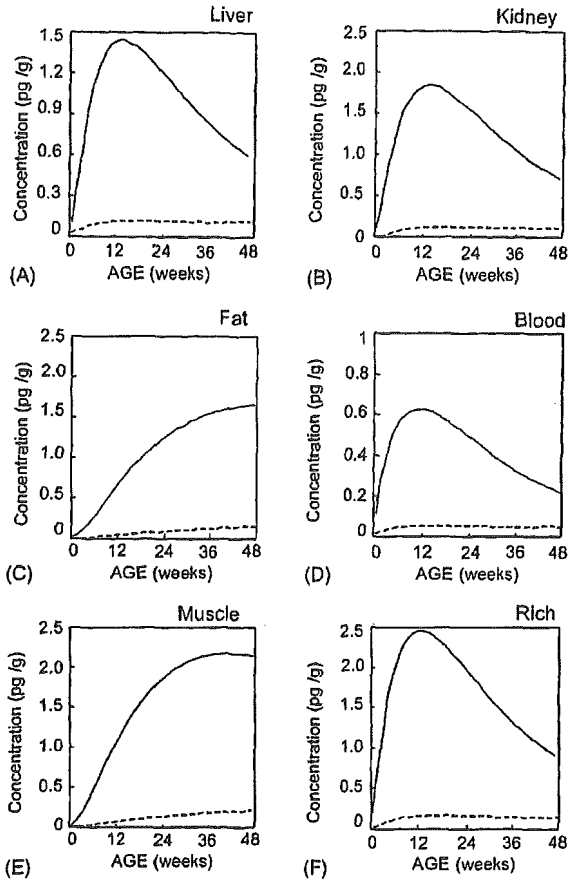

Fig. 4. Simulated concentrations (pg WHO-TEQ/g) of 2,3,7,8-TCDD in breast-fed (solid line) and formula-fed (broken line) infant liver (A), kidney (B), fat (C), blood (D), muscle (E) and richly perfused tissue (F).

3.3. Model validation

Dioxin concentrations in infant liver and blood were simulated using our model and the set of milk concentration data from publications (Table 3). Data source and simulation

Table 7
Simulated (Sim) and measured (Mes) concentrations in infant blood

	A1		A2		A3		A4		A5	
	Sim	Mes	Sim	Mes	Sim	Mes	Sim	Mes	Sim	Mes
2378-TCDD	0.08	0.02	0.07	0.01	0.07	0.02	0.10	0.02	0.06	0.01
12378-PeCDD	0.20	0.05	0.17	0.01	0.22	0.06	0.24	0.03	0.17	0.03
123478-HeCDD	0.26	0.04	0.25	0.01	0.29	0.06	0.37	0.00	0.26	0.04
123678-HeCDD	0.71	0.19	0.56	0.05	0.68	0.21	0.68	0.10	0.57	0.15
123789-HeCDD	0.09	0.03	0.08	0.01	0.13	0.05	0.11	0.02	0.11	0.05
1234678-HpCDD	0.53	0.11	0.49	0.13	0.62	0.26	1.11	0.08	0.93	0.16
OCDD	2.82	0.67	2.59	1.04	4.75	1.06	4.66	0.45	6.27	1.94
2378-TCDF										
12378-PeCDF										
23478-PeCDF	0.31	0.10	0.26	0.03	0.26	0.14	0.35	0.04	0.24	0.08
123478-HeCDF	0.23	0.04	0.23	0.02	0.24	0.05	0.31	0.04	0.23	0.04
123678-HeCDF	0.14	0.04	0.13	0.01	0.14	0.04	0.16	0.02	0.14	0.04
123789-HeCDF										
234678-HeCDF	0.27	0.02	0.28	0.0	0.28	0.02	0.35	0.01	0.29	0.01
1234678-HpCDF	0.43	0.06	0.65	0.04	0.41	0.04	0.37	0.02	0.50	0.10
1234789-HpCDF										
OCDF										
PCB77										
PCB81										
PCB126	4.82	1.29	4.64	0.21	7.02	1.68	10.6	0.51	7.64	0.64
PCB169	6.00	1.22	5.40	0.06	11.5	0.67	7.44	0.40	5.10	0.34
PCB105										
PCB114										
PCB118										
PCB123										
PCB156										
PCB157										
PCB167										
PCB189										

Measured concentration data are from American infants (Abraham et al., 1998).

conditions such as nursing term and point of sampling are listed in Table 4. The uptake of dioxin from baby food was based on Japanese babies and variations in food consumption behavior of babies in other countries were not included. Simulated concentrations were compared to the measured concentration data listed in Table 4.

Simulated and measured blood concentrations in American infants are listed in Table 7. In most of the congeners, simulated concentrations are 2–10 times larger than corresponding measured concentrations, except 2,3,4,6,7,8-HeCDF, 1,2,3,4,6,7,8-HpCDF, PCB126 and PCB169. In simulating adult tissue concentration, our model tends to overestimate 2,3,4,6,7,8-HeCDF concentration, and sometimes overestimate 1,2,3,4,6,7,8-HpCDF concentration, too. The overestimations for PCB126 and PCB169 are probably because these congeners are found in high concentration in Japanese fish and the uptake level from baby food was too high for American infants.

Simulated and measured concentrations in liver and fat are listed in Tables 8 and 9. In Table 8, simulated concentrations were within the range of measured concentrations in liver and fat, except that 4 simulated congeners in liver were overestimated. In Table 9, 90% of the ratios of simulated/measured concentrations were 0.1–10. From these results, our simulation data seems to show good agreement with the data in the literature.

The amounts of dioxin in infant feces are calculated as "$C_{liver} \times V_{liver} \times K_1$", and simulated and measured amounts in feces are listed in Table 10. The purpose of this simulation is to see whether the elimination route we set in our model can reasonably explain the actual elimination of dioxin in humans. A similar method for elimination via biliary excretion was also used in a previous model and validated in the literature (Kreuzer et al., 1997). In Table 10, we severely overestimated some data for 8 congeners (2,3,7,8-TCDD, 1,2,3,7,8-PeCDD, 1,2,3,4,7,8-PeCDD and 1,2,3,6,7,8-HeCDD), but most of the ratios between simulated and measured amounts are within the range 0.1–10 suggesting good agreement. From these results, our assumption of elimination route seems acceptable, although it might only work under the condition of the present level being low-dose and slow-elimination, and it might cause severe underestimation in an accidental high exposure. This assumption was similar to that by Kreuzer et al., and they

Table 8
Simulated (Sim) and measured (Mes) concentrations in infant liver (B1) and fat (B2)

	B1 (liver)				B2 (fat)			
	Sim	Mes			Sim	Mes		
		Avr	Min	Max		Avr	Min	Max
2378-TCDD	0.29	0.11	0.03	0.30	0.37	1.01	0.17	3.35
12378-PeCDD	6.22	0.34	0.07	0.91	7.26	3.89	0.34	12.0
123478-HeCDD	6.67	0.43	0.08	1.11	7.19	2.52	0.26	7.91
123678-HeCDD	27.5	1.24	0.20	3.51	30.1	12.2	1.81	31.8
123789-HeCDD	2.76	0.39	0.09	1.04	2.56	2.93	0.69	8.17
1234678-HpCDD	18.3	7.49	1.30	25.7	17.8	15.4	4.39	49.0
OCDD	108	79.4	24.4	190	99.1	97.9	37.0	293
2378-TCDF	1.57	0.11	0.07	0.20	1.78	1.00	0.43	2.67
12378-PeCDF	0.53	0.10	0.07	0.13	0.56	0.43	0.43	0.43
23478-PeCDF	10.5	1.47	0.21	5.33	11.9	7.44	1.38	28.4
123478-HeCDF	4.30	1.76	0.13	6.96	4.39	3.77	0.86	10.3
123678-HeCDF	4.18	1.96	0.19	5.53	4.93	2.38	0.60	8.00
123789-HeCDF								
234678-HeCDF	1.51	0.38	0.07	0.98	2.32	0.92	0.26	2.58
1234678-HpCDF	4.42	3.24	0.26	11.0	5.13	4.47	0.86	10.3
1234789-HpCDF								
OCDF	1.00	0.59	0.29	0.98	1.03	0.51	0.43	1.03

Measured data are from German infant tissues (Beck et al., 1994). Average (avr), minimum (min) and maximum (max) values were calculated by the authors based on the concentrations in the literature.

also validated their model by comparing simulated concentrations in liver, fat and feces to the corresponding tissue concentrations in previous reports (Kreuzer et al., 1997). We used the same assumption in an adult model and the model was validated using adult liver concentration (Maruyama 2et al., 2003). However, it is advantageous to validate it in an infant model, since the contribution of the background level in the liver is sufficiently low to be neglected in infants.

3.4. Effect of breastfeeding on the tissue concentrations in young people

To investigate the effect of breast milk on the tissue concentration in children, we simulated the time-course of dioxin concentrations for males of 1–20 years of age. Different model parameters were used for children, as described in Section 2. The calculated final concentrations in infant tissues were used as the initial concentrations in 1-year-old

Table 9
Simulated (Sim) and measured (Mes) concentrations in infant liver (C1, C2) and fat (C3, C4)

	C1		C2		C3		C4	
	Sim	Mes	Sim	Mes	Sim	Mes	Sim	Mes
2378-TCDD	0.10	0.04	0.23	0.36	1.60	0.11	3.12	0.28
12378-PeCDD	0.53	0.31	0.76	7.86	6.16	1.82	9.04	5.54
123478-HeCDD	0.58	0.52	0.71	8.24	4.40	1.87	7.60	5.54
123678-HeCDD	1.82	1.29	0.29	35.9	24.9	7.13	44.9	23.7
123789-HeCDD	0.38	0.28	0.84	3.07	3.36	0.76	10.8	1.91
1234678-HpCDD	12.3	1.60	7.20	20.7	14.1	5.08	61.6	13.1
OCDD	64.7	10.7	40.7	121	60.1	28.5	202	73.2
2378-TCDF	0.06	0.20	0.13	1.93	0.44	0.49	1.44	1.38
12378-PeCDF	0.07	0.08	0.05	0.62	0.70	0.17	0.48	0.42
23478-PeCDF	3.13	0.42	1.66	14.1	12.8	2.74	14.6	9.44
123478-HeCDF	4.01	0.39	0.88	5.10	4.24	1.20	6.00	3.28
123678-HeCDF	4.90	0.31	0.56	5.72	3.28	1.15	5.44	4.00
123789-HeCDF	0.01	0.04	0.06	0.00	0.04	0.04	0.10	0.00
234678-HeCDF	1.13	0.36	0.25	1.69	1.28	0.81	1.92	1.67
1234678-HpCDF	5.28	0.81	0.98	5.60	3.84	1.47	7.84	4.01
1234789-HpCDF	0.41	0.13	0.14	0.02	0.04	0.07	0.23	0.00
OCDF	1.00	0.47	0.70	1.10	1.12	0.46	1.76	0.74

Measured data are from German infant tissues (Kreuzer et al., 1997).

Table 10
Simulated (Sim) and measured (Mes) amounts excreted (pg/day) in infant feces

	D1		D2		E1		E2	
	Sim	Mes	Sim	Mes	Sim	Mes	Sim	Mes
2378-TCDD	6.18	0.63	9.40	1.34	5.63	1.18	3.25	1.64
12378-PeCDD	26.6	1.47	27.6	2.70	13.7	7.28	12.9	5.58
123478-HeCDD	23.7	1.85	31.2	7.07	7.78	4.06	7.65	3.45
123678-HeCDD	65.6	5.74	134	15.0	47.1	33.7	46.7	29.5
123789-HeCDD	16.1	2.99	14.1	7.90	2.47	6.79	2.59	6.17
1234678-HpCDD	39.9	13.4	137	88.2	26.0	96.3	26.9	110
OCDD	135	130	456	746	125	1118	130	984
2378-TCDF	2.96	1.87	17.0	3.52	3.86	1.61	4.12	1.37
12378-PeCDF	0.48	0.34	2.46	0.56	1.71	0.67	1.72	0.73
23478-PeCDF	9.95	1.39	69.4	6.85	37.6	15.2	35.5	11.9
123478-HeCDF	12.0	0.62	15.8	5.45	9.61	7.14	9.53	8.70
123678-HeCDF	11.9	1.16	24.9	4.70	10.6	8.91	11.7	6.71
123789-HeCDF	0.10	0.12	0.41	0.75				
234678-HeCDF	6.23	1.20	7.62	4.04	7.47	2.19	7.22	2.21
1234678-HpCDF	14.9	4.14	38.9	8.27	23.8	46.6	24.3	36.1
1234789-HpCDF	0.03	0.13	1.35	0.93				
OCDF					18.5	25.9	17.9	27.3

Measured data are from German (Korner et al., 1993) (D1 and D2) and American (Abraham et al., 1994) (E1 and E2) infants.

children's tissues. Simulated liver, fat and blood concentrations of breast-fed and formula-fed children's tissues were compared to the concentration range in corresponding adult tissues (Fig. 5). The high concentration that resulted from breast milk decreased rapidly after milk ingestion was stopped. The difference in concentration between breast-fed and formula-fed infants disappeared in 5–10 years in all tissues except fat. This is partly due to the decrease in dioxin uptake and the dilution of tissue concentration because of gaining of weight. Simulated concentration in the infant liver had a temporal high level at age 1 and this level was the same level as the maximum of the adult liver concentration range (Fig. 5A). The simulated concentration in infant fat was lower than the measured concentration in adult fat (Fig. 5B), while simulated infant blood concentration was more than 10 times higher than adult blood concentration (Fig. 5C). From these results, the ratios between adult and infant tissue concentrations are variable depending on each tissue. About the liver concentration, the level in infant liver seems to be in the range of that in adult liver, suggesting that the toxic effect to infant may not be severer than that to adult.

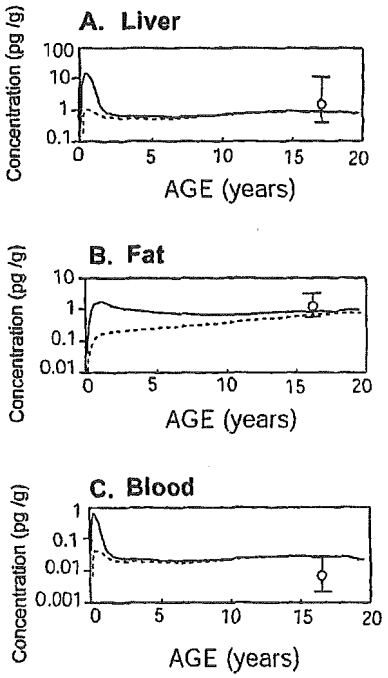

Fig. 5. Simulated liver (A), fat (B) and blood (C) concentrations for a man of 0–20 years of age. Solid lines are concentrations of breast-fed infant, and broken lines are those of formula-fed infant. Bars with a circle are the ranges of measured concentration in Japanese adults. The circle indicates the mean concentration.

3.5. Risk analysis of human infant

Kirman et al. (2000) proposed an improved method for cancer dose response characterization. Their approach is more sophisticated than the historical cancer slope factors used by the US EPA, since the method of Kirman is based on a mechanistic approach and the PBPK model is applied for route-to-route extrapolation. They showed that the pooled bioassay data could be utilized to obtain a dose–response model along with a PBPK model and applied their method to characterize the dose–response of acrylonitrile on brain tumors. Ayotte et al. simulated concentrations of 2,3,7,8-TCDD, PCB77, 126 and 169 in liver and fat in human infant, using a three-compartment model established by Carrier et al. (1995a,b), and compared simu-

lated liver concentration in a human infant to the measured liver concentration in a rat carrying liver cancer as reported in Kociba's study.

Aiming at a similar approach, we tried to estimate dioxin concentration in the target organ using a human PBPK model. In this study, we focused on the infant liver, since concentration data are usually available for blood, fat and liver in the literature, and the relationship between dioxin exposure and the formation of hepatic foci in liver is studied from the mechanistic point of view (Pitot et al., 1980; Portier et al., 1996; Tritscher et al., 1992). Although the liver concentration may not be appropriate dosimetry for non-cancer risk such as immune toxicity and developmental toxicity, we used the liver concentration to non-cancer assessment.

To analyze the relative risk of dioxins in breast-fed infants, we compared simulated liver concentrations in human infants and adults with the concentrations that were associated with toxicity in rats (Table 5). Relative risk values were calculated as the ratios of liver concentrations between rat and human.

Simulated maximum, minimum and mean concentrations for a breast-fed infant were 16.8, 0.95 and 11.5 pg H4IIE-TEQ/g tissue, respectively. The maximum, minimum and mean concentrations for a formula-fed infant were 3.51, 0.18 and 2.89 pg H4IIE-TEQ/g tissue, respectively. In Kociba's report, liver concentration of 2,3,7,8-TCDD in a rat with liver cancer was 24,000 pg/g (= 24,000 pg H4IIE-TEQ/g), and liver concentration in a rat with liver lesions (related to liver cancer) was 5100 pg/g (= 5100 pg H4IIE-TEQ/g). Therefore, we selected 5100 pg/g as a LOAEL for liver cancer, and the relative risk to breast-fed and formula-fed infants were approximately 1/300 and 1/1460, respectively. Teeguarden et al. (1999) reported cancer promotion activity of 2,3,7,8-TCDD in diethylnitrosoamine (DEN)-treated rat. In their report, formation of altered hepatic foci increased at dose 10 ng/kg BW day, biweekly intraperitoneal administration after partial hepatectomy. According to Tritscher's study (1992) liver concentration after biweekly oral administration at dose 10.7 ng/kg BW day was 1.67 ng/g tissue. From these data, the LOAEL of liver concentration for cancer promotion activity is 1670 pg/g, although the routes of dioxin administration to rats are different in Teeguarden's and Tritscher's studies. Relative risks for cancer promotion from this concentration were 1/100 and 1/480 for breast- and formula fed infants, respectively.

About non-cancer risks, there are fewer concentration data sufficient for risk assessment. Faqi et al. reported a reduction in sperm number in pups whose mother received 25 ng/kgBW of initial dose and 5 ng/kgBW of weekly maintenance dose (Faqi et al., 1998), and they suggested liver concentrations in maternal (75 pg/g) and offspring (240 ng/g) liver. Gray et al. reported that 1 μg/kgBW of TCDD administration at gestational day 15 (GD15) caused reduction of fertility in the next generation (Gray et al., 1995) and 50 ng/kgBW of TCDD administration at GD15 caused delayed eye opening and reduction of sperm number in the next generation (Gray et al., 1997). Hurst measured maternal and fetal liver concentrations after the same TCDD administration to a pregnant rat as in Gray's study (Hurst et al., 2000), and the maternal and fetal liver concentrations were 368 and 6.2 pg/g, respectively.

The relative risks of reproductive toxicity calculated from maternal liver concentration in Faqi's study were 1/5 and 1/21 for breast- and formula fed infants, respectively, and the risks calculated using Gray's data were approximately 1/22 and 1/105 for breast- and formula fed infant, respectively. According to these results, the internal level for human infant may be close to the level in rat associated to reproductive risk.

Although it seems inappropriate to compare the concentration in human infant to the concentration in adult rat, there is no other concentration data available for better reference. Gray's and Ohsako's studies should be referred in assessing reproductive toxicity, since the present TDI of dioxin is based on the dose in their reports. When the simulated liver concentration in human aged 17–20 (1.0 pg H4IIE-TEQ/g) is referred to the maternal concentration in Gray's study, the relative risk is reduced to 1/368. This is considerably low and seems inconsistent with the ratios between TDI (4 pg TEQ/kg BW day) and the present uptake level (2 pg TEQ/kg BW day). There is no other report on toxicity versus internal concentration in rat infant. To determine the risk level quantitatively, critical age, target tissue and the tissue concentration are required both for animals and humans.

4. Discussion

Some researchers have estimated the internal concentration in a human infant using mathematical models. Most of those models are one to three compartment models, and the obtained results are body burden or the concentrations in fat and liver. An advantage of our model is that seven compartments are taken into account and detailed concentration changes in various target tissues are available. For example, the previous models did not estimate concentration in brain or reproductive organs, although we need to consider these tissue as the target organs for neurotoxicity and reproductive toxicity. We set richly perfused tissue as a substitute for lung, brain and spleen, and this concentration can be substituted for the concentration in reproductive organs, since measured concentrations in the human brain are similar to those in the human ovary and testis (Environment Agency, 2000). A demerit of our model is that it might not estimate liver concentration fully after accidental high exposure, because our model lacks a component for induction of binding protein in the liver. If sufficient information about the concentrations of CYP1A1 and CYP1A2 in the human liver is available, this parameter can be introduced in our model.

We have presented only simulation patterns of 2,3,7,8-TCDD in our figures, but concentrations of all 29 dioxin congeners were studied and their time-dependent patterns were similar to those observed in 2,3,7,8-TCDD concentration (data not shown). Our simulated pattern of time-dependent change in tissue concentration is similar to the patterns observed in infant body burden and tissue concentration in previous reports (Ayotte et al., 1996; Kreuzer et al., 1997; Lakind et al., 2000). Ayotte et al. simulated liver and fat concentration of 2,3,7,8-TCDD, and their simulated concentration in liver in the WHO-TEQ basis had a peak at age 1 and decreased to the lowest level at age 10. According to our results, decrease in concentration to the basal level was observed at an early age (age five), and this is probably because of a difference in method of calculation from that in the model used by Ayotte et al. Using their estimation, Ayotte et al. compared the simulated liver concentration to the measured concentrations in rat liver in Kociba's study for cancer risk assessment. A similar risk assessment method using tissue concentration was proposed by Kirman et al. (2000), and Kirman characterized the dose–response relationship of acrylonitrile on brain tumors.

In the risk assessment, no-observed adverse effect level (NOAEL) is generally used to set tolerable daily intake (TDI) or the margin of exposure (MOE). Safety factor (usually 3–10) is also taken into account, and the risk is calculated by present exposure times safety factor divided by TDI. This assessment result means that how far the present exposure is from NOAEL and safe. In the case of dioxins, the present level may not be sufficiently safe especially for the next generation according to the NOAEL obtained from animal studies (Gray et al., 1995; Ohsako et al., 2001). Therefore it may not be practical to calculate a margin of "safety" using NOAEL. We are trying to calculate the probability of suffering a toxic effect using the LOAEL found in the literature. The probability of toxicity indicates how dangerous the present level is. Its merit is that we can know and characterize risk potential and prepare for a probable toxic effect in the future. It can also suggest quantitative information to risk management using risk/benefit and cost/benefit analysis, since this kind of information can be useful to calculate the social cost.

The schematic view of risk characterization is shown in Fig. 6. For quantitative risk assessment, accurate interspecies extrapolation and route-to-route extrapolation should be performed based on the concentration at the target organ (Tissue A). Route-to-route extrapolation and interspecies extrapolation are often required, since available bioassay data are not usually uniform in their route and term of exposure or dose level. For this purpose, the PBPK model is most appropriate to estimate concentrations not only in Tissue A but other tissues for pool or elimination of the compound (tissue B, C, etc.). Dose–response characterization should be analyzed at the target organ, and unit risk or excess risk can be calculated using the benchmark dose method (Crump, 1995).

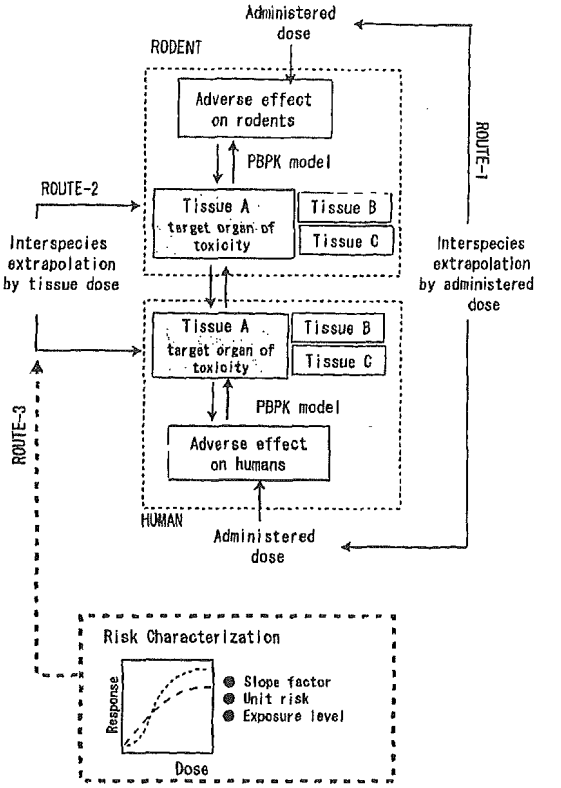

Fig. 6. Schematic diagram of quantitative risk assessment of dioxin to humans. Tissue A indicates the target organ in which dose versus toxic response should be considered based on a mechanistic model. Tissues B and C are non-target but important tissues to consider ADME. Shadowed areas (tissue A) are rat and human livers in this study. ROUTE-1 is interspecies extrapolation based on the administered dose of dioxin. ROUTE-2 is interspecies extrapolation based on tissue dose, which is measured or estimated with the PBPK model. ROUTE-3 is the method used for calculating unit risk or slope factor.

Historically, in risk assessment for humans, unit risk (unit dose versus excess risk) was obtained from epidemiology data and risk (probability of adverse effect) is calculated by multiplying unit risk and exposure (dose) level. The demerit of using epidemiology data is that too many unknown factors are included in the data and they cannot be separable from the effect of the target chemical. If the interspecies extrapolation method is reliable and dose–response data at the target organ is available, bioassay-based assessment is more accurate for predicting health risks to humans. In ROUTE-1 (Fig. 6), uncertainty is apparently larger than in ROUTE-2, since interspecies differences such as half-life and tissue volumes are not taken into account. The US EPA calculated the cancer slope factor for dioxin using body burden of experimental animals and benchmark dose (BMD) in their final report (US EPA, 2000). This is an intermediate method between ROUTE-1 and ROUTE-2, since body burden is a kind of tissue dose approved by EPA. We tried to improve the EPA's method, by introducing tissue dose estimated with

our PBPK model in this study, although our results are still not sufficient for quantitative risk assessment.

Risk assessment for infant and child has been tried by several researchers using epidemiology data. For example, Rogan et al. (1991) analyzed the cancer risk of infants and found no clear differences between breast- and formula-fed infants. Pluim et al. (1994) reported a difference in infant plasma aminotransferase levels. Nagayama et al. (1998) reported different thyroid hormone levels in Japanese breast-fed infants, although their results seem unclear. Hoover (1999) assessed the health risk to infants using an exposure analysis of organochlorines that included dioxins and PCBs. Despite these studies, differences in health status between breast-fed and formula-fed infants are still not clear, probably because the present contamination level is not severe enough to make a distinct difference between exposed and unexposed groups in an epidemiology study. Bioassay-based risk assessment is more sensitive for detecting a subtle adverse effect, but the absence of appropriate methodologies for interspecies extrapolation is a critical point at present.

Our model can be applied to assessing quantitative health risks to humans, but information about the toxicity of dioxin to humans is still limited in quantity, especially on infants and children. For example, the cumulative exposure of a chemical is taken into account on cancer risk and the area under the concentration curve (AUC) is used as dosimetry, while AUC is not used in non-cancer assessment. In the case of dioxins, the relationships are not known quantitatively between effect and dose, AUC and tissue concentration. In order to assess health risk quantitatively, we need information concerning (1) the amount of chemical at the target tissue, (2) time of exposure and (3) doses that cause toxicity.

Nevertheless, our PBPK model distinguished different temporal patterns of dioxin concentration among tissues, which other previous studies did not. The transient high concentrations in liver, kidney, and richly perfused tissue on the 12th–24th weeks may be associated with adverse effects. For example, immunoglobulin (Ig) G decreases rapidly after birth and is at the lowest level around 3 months of age (the 12th week) (McClelland et al., 1978; Ogawa et al., 2000). Dioxin concentrations reach their peak at this time in many tissues (Fig. 4A, B, E, and F). Ig A, which protects the newborn from bacterial infections, is supplied from the maternal body during nursing. We noticed a possible effect on immune function in breast-fed infants, because the peak dioxin concentration in infant tissue coincided with decreased immunoglobulins (Fig. 4) (McClelland et al., 1978; Ogawa et al., 2000). Several researchers have reported relationships between TCDD exposure and virus infection (Yang et al., 1994), nematode infection (Luebke et al., 1994) and decrease in immunoglobulin producing cells (House et al., 1990) in mice. Weisglas-Kuperus et al. (2000) found that the number of lymphocytes and T-cells, lower antibody levels to mumps, and occurrence of measles were associated to the level of prenatal exposure of PCB. We did not assess risk to immune function in this study; however, we believe that more attention should be given to the physical conditions of infants, since their immune and metabolic systems may not be sufficient compared to those of adults.

Acknowledgements

The authors express gratitude to Professor Junko Nakanishi for her support for this study. We are also grateful to Professor Melvin E. Andersen and Professor Raymond S.H. Yang for their suggestions and advice on our PBPK model. This study was partially supported by Health Science Research Grants from the Ministry of Health, Labour and Welfare of Japan.

References

Abraham, K., Krowke, R., Neubert, D., 1988. Pharmacokinetics and biological activity of 2,3,7,8-tetrachlorodibenzo-p-dioxin. Arch. Toxicol. 62, 359–368.

Abraham, K., Wiesmuller, T., Brunner, H., Krowke, R., Hagenmaier, H., Neubert, D., 1989. Elimination of various polychlorinated dibenzo-p-dioxins and dibenzofurans (PCDDs and PCDFs) in rat faeces. Arch. Toxicol. 63, 75–78.

Abraham, K., Hille, A., Ende, M., Helge, H., 1994. Intake and fecal excretion of PCDDs, PCDFs, HCB and PCBs (138,153, 180) in a breast-fed and foprmula-fed infant. Chemosphere 29, 2279–2286.

Abraham, K., Papke, O., Gross, A., Kordonouri, O., Wiegand, S., Wahn, U., Helge, H., 1998. Time course of PCDD/PCDF/PCB concentrations in breast-feeding mothers and their infants. Chemosphere 37, 1731–1741.

Andersen, M.E., Mills, J.J., Gargas, M.L., Kedderis, L., Birnbaum, L.S., Neubert, D., Greenlee, W.F., 1993. Modeling receptor-mediated processes bwith dioxin: implications of pharmacokinetics and risk assessment. Risk Anal. 13, 25–36.

Andersen, M.E., Eklund, C.R., Mills, J.J., Barton, H.A., Birnbaum, L.S., 1997. A multicompartment geometric model of liver in relation to regional induction of cytochrome P450s. Toxicol. Appl. Pharmacol. 144, 135–144.

Andersen, M.E., Dennison, J.E., 2001. Mode of action and tissue dosimetry in current and future risk assessments. Sci. Total Environ. 274, 3–14.

Ayotte, P., Carrier, G., Dewailly, E., 1996. Health risk assessment for inuit newborns exposed to dioxin-like compounds through breast feeding. Chemosphere 32, 531–542.

Beck, H., Kleeman, W.J., Mather, W., Palavinskas, R., 1994a. PCDD and PCDF levels in different organs from infants II. Organohalogen Comp. 21, 259–264.

Beck, H., Dross, A., Mathar, W., 1994b. PCDD and PCDF exposure and levels in humans in Germany. Environ. Health Perspect. 102, 173–185.

Carrier, G., Brunet, R.C., Brodeur, J., 1995a. Modelings of the toxicokinetics of polychlorinated dibenzo-p-dioxins and dibenzofurans in mammalians, including humans. I. Nonlinear distribution of PCDD/PCDF body burden between liver and adipose tissues. Toxicol. Appl. Pharmacol. 131, 253–266.

Carrier, G., Brunet, R.C., Brodeur, J., 1995b. Modelings of the toxicokinetics of polychlorinated dibenzo-p-dioxins and dibenzofurans in mammalians, including humans. II. Kinetics of absorption and disposition of PCDDs/PCDFs. Toxicol. Appl. Pharmacol. 131, 267–276.

Crump, K.S., 1995. Calculation of benchmark doses from continuous data. Risk Anal. 15, 79–89.